Department of Physics and Astronomy
University of Heidelberg

Bachelor thesis
in Physics

submitted by
Alexander Mil
born in Rudnja (Russia)

Issued 2013

Realization of an amplified optical beating for bichromatic cooling of metastable argon

This bachelor thesis has been carried out by Alexander Mil at the
Kirchhoff Institute for Physics
under the supervision of
Prof. Dr. M. K. Oberthaler

Realization of an amplified optical beating for bichromatic cooling of metastable argon

This thesis presents the generation and amplification of a laser light beating. This is the first step towards the realization of bichromatic cooling for the Ar^{39}-ATTA experiment.

In the course of this thesis an experiment was set up to generate an optical beating using an acousto-optic modulator in double-pass configuration. Furthermore, a tapered amplifier device (TA) was built to amplify this beating. The device was characterized and succesfully used for amplification. The intensity of the beating was monitored to measure its parameters and to compare it with theoretical predictions. This way it could be shown that the TA amplifies the beating signal without detrimental effects on either phase or visibility.

Realisierung einer verstärkten optischen Schwebung für bichromatisches Kühlen von metastabilem Argon

Im Rahmen dieser Arbeit wurde mit Laserlicht eine optische Schwebung erzeugt und diese mit einem Trapezverstärker verstärkt. Dies stellt den ersten Schritt dar hin zu einer Realisierung von bichromatischem Kühlen für das ^{39}Ar-ATTA Experiment.

Im Rahmen dieser Arbeit wurde ein Experiment zur Erzeugung eines optischen Schwebung mit einem Akustooptischen Modulator in Doppel-Pfad-Konfiguration aufgebaut. Des Weiteren wurde ein Trapezverstärker (TA) aufgebaut, um diese Schwebung zu verstärken. Der optische Verstärker wurde charakterisiert und erfolgreich zur Verstärkung eingesetzt. Die Intensität der Schwebung wurde aufgenommen um ihre Parameter zu messen und diese mit theoretischen Vorhersagen zu vergleichen. Auf diese Weise konnte gezeigt werden, dass der TA das Schwebungssignal ohne abträglichen Einfluss auf Phase und Kontrast verstärkt.

Contents

1 Introduction

Radiative cooling is a standard laser technique for slowing down atoms. It has a wide range of applications in atomic physics such as the magneto optical trap (MOT), the Zeeman-slower and the collimation of atom beams. However, the radiative force is limited by the spontaneous decay rate of the atomic transition. Therefore, slowing down an atom requires a minimum cooling distance on the order of several decimeters for collimation up to several meters for Zeeman-slowing.
In certain experimental situations atoms have to be slowed down within a few millimeters, which is the case in the ^{39}Ar-ATTA experiment, where this thesis was carried out. There, a large velocity class of atoms needs to be collimated for obtaining high ^{39}Ar-counting rates. The collimation has to take place in a short distance in order to avoid a spatial spread of the atom beam.
Bichromatic cooling is a different cooling mechanism that overcomes the limitation of radiative cooling given by the spontaneous decay rate. Instead of absorption followed by spontaneous emission bichromatic cooling is based on absorption followed by stimulated emission. These absorption-emission cycles can be arbitrarily fast only limited by available laser power. The bichromatic force can therefore exceed the radiative force by factors up to an order of magnitude.
The objective of this thesis is the realization of an amplified optical beating to drive these absorption-emission cycles which represent the key ingredient for bichromatic cooling.
In the following the crude basics of bichromatic cooling will be illustrated using the simplifying π-pulse model. Subsequently its possible application in the ^{39}Ar-ATTA experiment is discussed and rough design parameters are estimated.

1.1 Basics of bichromatic cooling

The concept of the π-pulse model is shown in figure 1.1. An atom is exposed to two amplitude modulated light beams with carrier frequency ω_a and modulation (or beat) frequency $\Delta\omega$ propagating in opposite direction. The carrier frequency is tuned to atomic resonance. Then the modulation frequency and the intensity of the beams are chosen such that these beams can act as a sequence of π-pulses [1]. A π-pulse induces a half rabi cycle in a two-level atom, meaning it coherently drives the population from ground to excited state and vice-versa. The π-pulse condition yields $\Omega_{rabi} = \pi\Delta\omega/4$ [2], with the Rabi frequency given by

$$\Omega_{rabi} = \gamma\sqrt{\frac{I_0}{2I_s}} \quad , \tag{1.1}$$

where γ is the linewidth of the transition between ground and excited state, $I_0 \propto |E_0|^2$ the laser intensity, I_s is the saturation intensity and E_0 the electric field of the light.

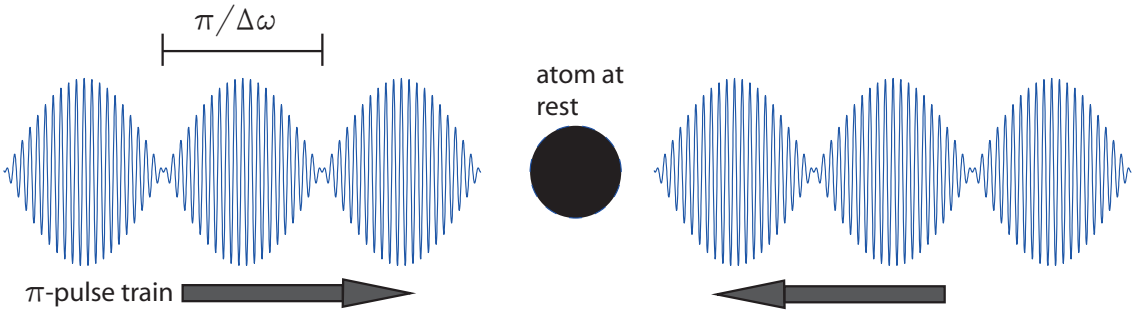

Figure 1.1: Sketch illustrating the π-pulse model of the bichromatic force.

When the π-pulse condition is fulfilled, the beams act as π-pulse trains with each π-pulse having a period of $\pi/\Delta\omega$ [1]. The idea is to shift the phase of both beams such that the π-pulse coming from the left drives the atom to the excited state via absorption directly followed by the π-pulse coming from the right that drives the atom back into the ground state via stimulated emission. This causes a net momentum exchange of $2\hbar k$ to the right. Due to spontaneous emission the optimal phase between the two counterpropagating pulse trains turns out to be $\pi/2$. Changing the phase shift between the pulses to $3\pi/2$ reverses the direction of the force. The net force on the atom resulting from coherent momentum exchange (and taking into account spontaneous emission) can be deduced to [1]

$$F_B = \frac{\hbar k \Delta\omega}{\pi} = \frac{4\hbar k \Omega_{rabi}}{\pi^2} \tag{1.2}$$

This force exceeds the maximum radiative force by a factor of $2\Delta\omega/\pi\gamma$, which can be huge since Ω_{rabi} is only limited by the available laser power.
The considerations of the π-pulse model so far give an intuitive understanding for the origin of the bichromatic force. However, this model is somewhat inaccurate. It does not take into account the temporal overlap of the pulses. Furthermore the π-pulse condition does not take into account the changing Doppler shift during the slowing process.
A more rigorous derivation for the origin of the bichromatic force can be done in the doubly dressed atom picture. It yields the optimum Rabi frequency to be $\Omega_{rabi} = \sqrt{\frac{3}{2}}\Delta\omega$, which is different from the expression obtained with the *pi*-pulse model. For detailed information the interested reader is advised to [1] and [2].

The models only describe the physical origin of the bichromatic force and give estimates for the optimal laser parameters $\Delta\omega$ and Ω_{rabi}. More detailed information can be achieved by numerical calculations based on solving the optical-Bloch-equations. The results of such a calculation is presented in figure 1.2. The force is centered around $v = 0\frac{m}{s}$ and has a velocity range $\Delta v \approx \Delta\omega/k$.

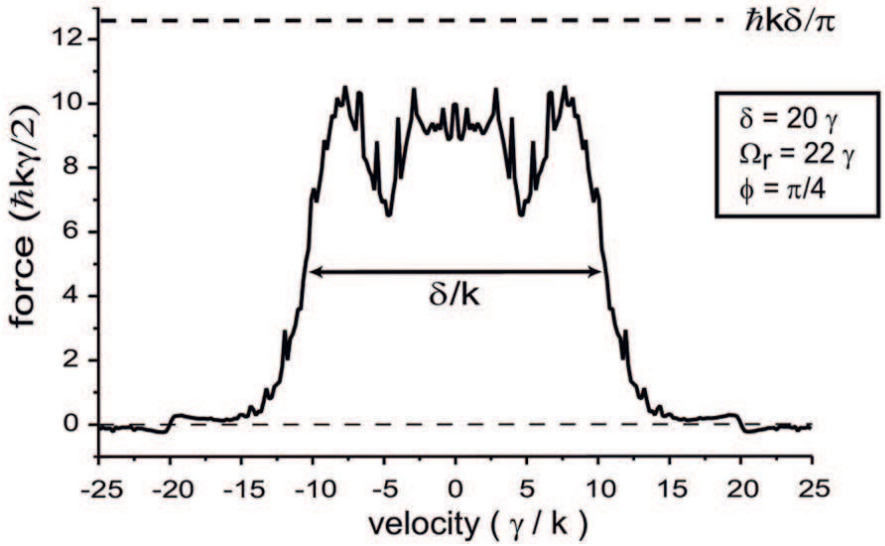

Figure 1.2: Numerical calculation of the bichromatic force as a function of atom velocity for a fixed detuning. The used parameters are shown in the plot. The force axis is in the units of the radiative force. Note that δ represents $\Delta\omega$ above. Picture taken from [3].

To change the velocity class of atoms addressed by the bichromatic force the center of the force has to be shifted. This can be achieved by adding the frequency $\pm kv_c$ to the atomic transition frequency ω_a of the beams to compensate for the Doppler shift. In the frame of an atom moving with velocity v_c the counterpropagating beams appear to be the same as in the simplified case above.

1.2 Possible application in ATTA

The part of the ATTA experiment that would benefit from a bichromatic cooling setup is the collimation of the ^{39}Ar beam right after it leaves the source tube. To make ^{39}Ar applicable for cooling and trapping it has to be excited in a certain state [4]. This is done via a RF-discharge in the source tube. The collimator is needed to slow down the transverse velocities of the argon beam, so it can pass the rest of the apparatus and finally reach the MOT, where the atoms are detected. To make exact statements about the collimation process one has to take into account many details and properties of both excitation source and collimator. To obtain a rough estimate for the design parameters of the bichromatic cooling setup a "back-of-the-envelope"

like calculation is presented in the following.
Figure 1.3 shows a sketch of the collimation geometry.

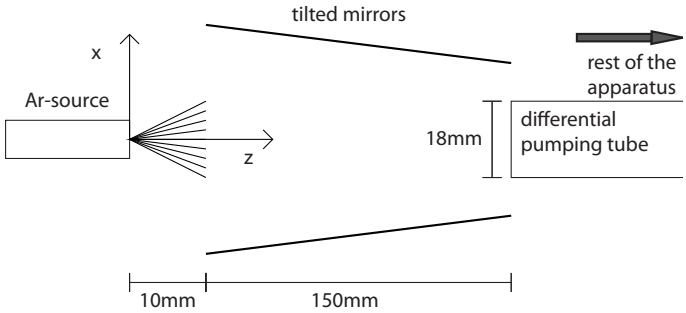

Figure 1.3: Sketch of the collimator in the ATTA experiment (not to scale)

The source is cooled with liquid nitrogen and it is assumed that the atoms arise from the point of origin and have a mean longitudinal velocity $v_l = 274\frac{m}{s}$. Further it is assumed that the atoms passing the collimator mirrors receive a mean accelaration $a = 1 \times 10^5 \frac{m}{s^2}$ (half the maximum acceleration). The maximum transverse velocity is determined for which the atoms still reach the MOT. To reach the the rest of the apparatus the atoms have to pass the differential pumping tube so the restrictions for the maximum transversal velocity are: The atom with maximum transverse velocity after passing the collimation can only be displaced by 9mm from the z-axis and has to have vanishing transverse velocity. So classical mechanics yield

$$x_{max} = v_{max}t_{1cm} + v_{max}t_0 - \frac{1}{2}at_0^2 \stackrel{!}{=} 9mm \qquad , \tag{1.3}$$

where t_{1cm} is the time the atoms spend in the first stretch of 1cm and t_0 is the time it takes the collimater to slow the transversal velocity down to 0. It is assumed that the atoms receive a constant decelaration until the transverse velocity vanishes (a strongly simplified assumption since the radiative force is velocity dependent).
Inserting the numbers in equation 1.3 yields $v_{max} \sim 40\frac{m}{s}$ and the transverse displacement d_{max} from the z-axis gained by the atom while passing the first strech of 1cm is 1.5mm.
Now the possible effects of bichromatic cooling are estimated. Such a possible setup would consist of two counterpropagating beams covering the space right before the collimator (see figure 1.4).

With $\Delta\omega = 2\pi \times 60$MHz and the excited Argon properties $\gamma = 2\pi \times 5.87$MHz and $I_s = 1.44\frac{mW}{cm^2}$ [2] this yields a needed laser power of $\sim$ 450mW for each beam (assuming both beams have a cross section of 1cm^2).
The arising bichromatic force has an approximate constant acceleration of $1.5 \times 10^6 \frac{m}{s^2}$ over a velocity range $\Delta v = 50\frac{m}{s}$. The impact of the bichromatic force on the collimation process depends on the velocity class to which the center of the force is shifted. When shifting the center of the force to $\sim 65\frac{m}{s}$ so that within the 1cm stretch all velocity classes up to $\sim 90\frac{m}{s}$ are decelerated down to $40\frac{m}{s}$, the atoms will reach

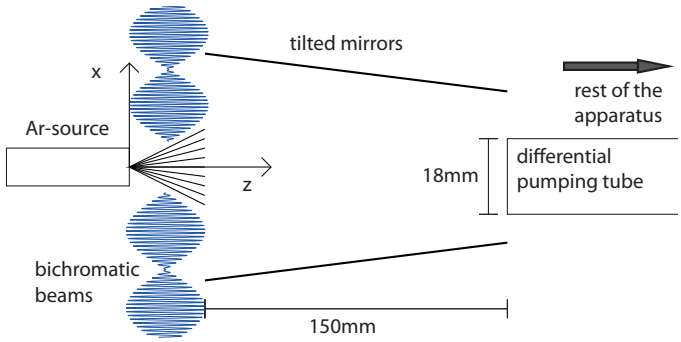

Figure 1.4: Sketch of the collimator with indicated beams for the bichromatic cooling (not to scale)

the collimator with a velocity that can be slowed down to zero by the collimator. However, the atoms would gain bigger transversal displacement than d_{max} and may not reach the differential pumping tube. So a trade-off choice would be to shift the center of the force to $45\frac{m}{s}$. In that case all atoms up to $\sim 70\frac{m}{s}$ are slowed below the maximum capturing velocity of the collimator while getting less displacement than d_{max}.
Summing up, the implementation of a laser cooling scheme based on the bichromatic force could approximately double the transversal velocity range of atoms that can be detected with the apparatus.

2 Tapered Amplifier

As calculated in section 1.2 two amplitude modulated laser beams with ∼450 mW power each have to be generated for an application of bichromatic cooling. Since the usual output powers of the used diode laser systems are below 100mW the laser power has to be amplified (as shown in figure 2.1).To obtain a laser beam that can be used as a π-pulse train, two steps are considered. In the first step an optical setup is used to create an amplitude modulated signal. In the second step a Tapered Amplifier (TA) is used to amplify the signal to reach the necesssary output power. This chapter describes the TA that was built in the course of this thesis.

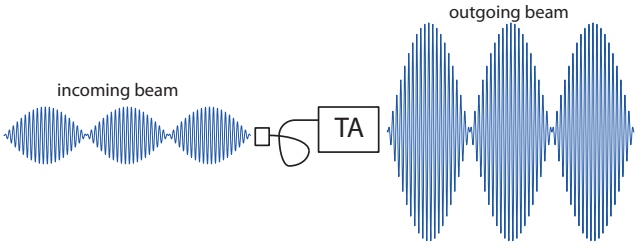

Figure 2.1: Sketch of the basic concept of amplifying an optical beating with a TA.

2.1 Basic functionality

The TA laser diode acts similar to usual laserdiodes i.e. it is a semiconductor element that is driven with a current. In the usual operating mode, a laser beam is focused onto the TA diode, which amplyfies this seed beam while maintaining its properties such as frequency or modulation. The TA diode has two important features.

The first one is that both facets of the TA diode are antireflex coated thus there is no roundtrip oscillation in the cavity and the wavelength of the output beam is mainly determined by the seed laser. The second pecularity of the TA diode is its geometry. As one can see from figure 2.2 the output end of the diode is tapered, thus allowing the beam power to spread over the active region. By that a TA can run at high output power without taking damage due to excessive heating at the output facet. The used TA diode was purchased from Eagleyard (Part-No.: YP-TPA-0808-01000-4006-CMT04-0000, Serial No.: EA-00881).

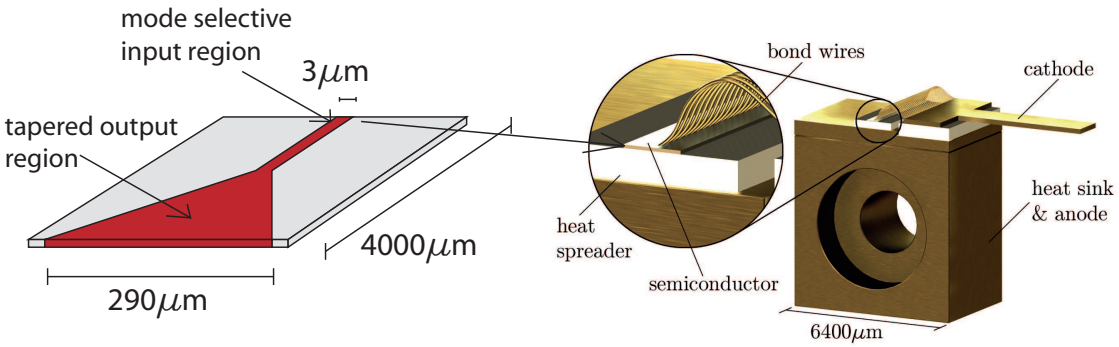

Figure 2.2: Left: Sketch of the TA diode (not to scale). Right: Technical drawing of the TA chip. The middle hole is used for mounting with a screw and also provides electrical ground. In the detailed view the semiconducter diode can be seen.

2.2 Mechanical setup

Figure 2.3 provides a picture of the self-built TA device and a detailed sketch of the needed optics. The whole system is mounted on an aluminum block that is cut in two pieces. Peltier elements are placed in between these two parts. The peltier elements are driven by a temperature controller that has also been built in the course of this thesis to ensure a constant temperature of the device.

The TA is operated with a laser diode controller (Thorlabs LDC 240C). The ports for both temperature and current control are SUBD9 ports. They can be seen on the right side of the picture.
Below is a brief summary of the needed optics and the way they are used in the setup.

- **Fiber coupler + right angle kinematic mirror:** The fiber coupler collimates the seed laser and the right angle kinematic mirror deflects the beam. Since both are mounted on mirror mounts that can be tilted in two different angles, they provide the four degrees of freedom to align the incoming beam, so that it can be focused onto the front facet of the TA diode.

- **Half-wave plate:** The performance of the TA diode is polarization dependent. The half-wave plate is needed to rotate the polarization axis of the seed laser so that it matches the condition of the TA diode. The incoming fiber has to be coupled polarization maintaining to avoid power fluctuations

- **Focussing aspheric lens:** The magnitude of the front facet of the TA diode is on the order of a few mikrometers whereas the incoming seed laser has a beam diameter of a few milimeters. In order to match both dimensions a lens is needed that focuses the incoming seed laser beam onto the facet of the TA diode. The lens can be adjusted in all three dimensions.

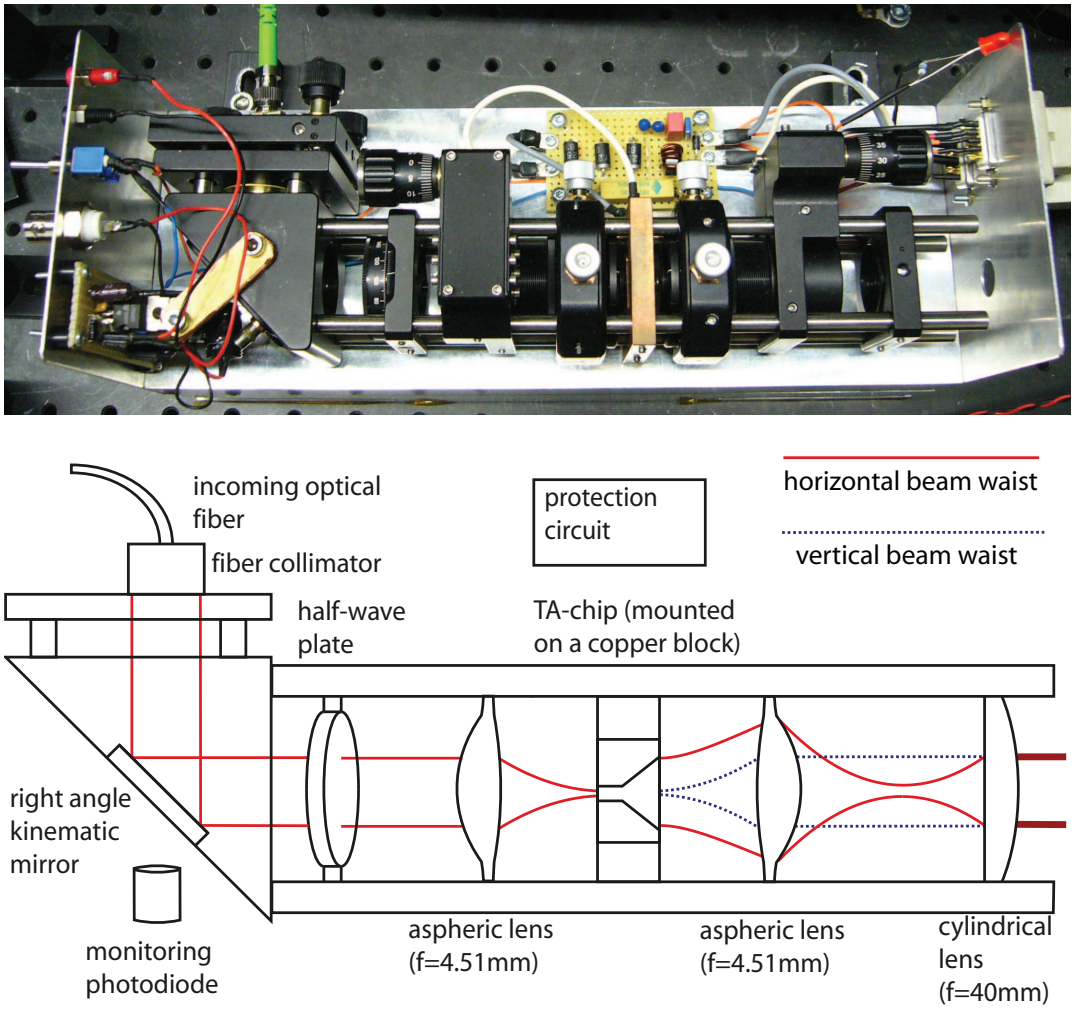

Figure 2.3: Top: Picture of the real TA device that was set up in the laboratory. Bottom: Sketch of the mechanical setup and the needed optics (not to scale). The path and the beam waist of the incoming and outgoing beam is also depicted.

- **Collimating aspheric lens + cylindrical lens:** The vertical and horizontal component of the output beam at the rear facet of the TA have different divergency as well as different beam diameters. The strongly divergent vertical beam component is collimated by the aspheric lens while it remains uneffected by the cylindrical lens. The less divergent horizontal beam component is collimated and shaped by the combination of aspheric and cylindrical lens. Past the cylindrical lens both horizontal and vertical beam waist should match in a proper manner.
  The aspheric lens can be adjusted in all three dimensions. The cylindrical lens can be adjusted in the direction of the beam.

2.3 Characterization

In order to characterize the TA several of its properties were measured. These measurements include the dependency of the TA output power on seed laser power and injection current. Furthermore the dependency of the seed monitoring photodiode as a function of seed laser power was measured. It must be noted that for the purpose of characterising the performance of the TA all measurements were carried out in a coarse manner.

2.3.1 Power

Since the TA setup has been built for the purpose of enhanced output power, this is obviously an important criterion. All power measurements below were carried out with a powermeter (Coherent FieldMate). For higher power the powermeter loses its linear response, hence for every measurement of a power exceeding 30mW an attenuator (Coherent Attenuator, Attenuation measured to be 1:778) was placed right before the powermeter.
The dependence of the TA output power on the injection current and on the seed laser power is shown in figure 2.4. In the left plot a laser threshold can be seen around 1000mA. Over 1700mA there is a linear increase in output power. One would also expect a linear dependence towards the maximum current value of 3000mA, but since the TA chip is a sensitive element for the time being no current injection above 2000mA was performed to prolong the lifetime of the diode.

The data points in the right plot show a slight saturarion effect towards higher seed laser power. According to [5] the output power P_{out} can be described by the following formula

$$P_{out}(P_s) = \frac{P_{max} \cdot P_s}{P_{1/2} + P_s} \quad , \tag{2.1}$$

where P_s is the seed laser power, P_{max} the maximum power and $P_{1/2}$ the seed laser power for which half of P_{max} is reached. The straight line in the right plot of figure 2.4 is a fit of that type. It yields P_{max}=534mW and P_s =9mW. In the present setup the seed laser power was delivered by an ECDL (Extern Cavity Diode Laser). The optical setup used to create a light beating strongly reduced the power of the laser beam, thus some measurements presented in 3.3 were carried out with only 1.5mW seed power.

Since the seed originates from a single mode optical fiber, its power critically depends on the fiber coupling efficiency. Therefore a photodiode has been placed behind the right angle kinematic mirror to monitor the seed laser power. The photodiode detects the small amount of light that is transmitted through the mirror. This way one can monitor the output power of the fiber without detaching it from the TA device.
It turned out that the transmission of the right angle kinematic mirror is very low.

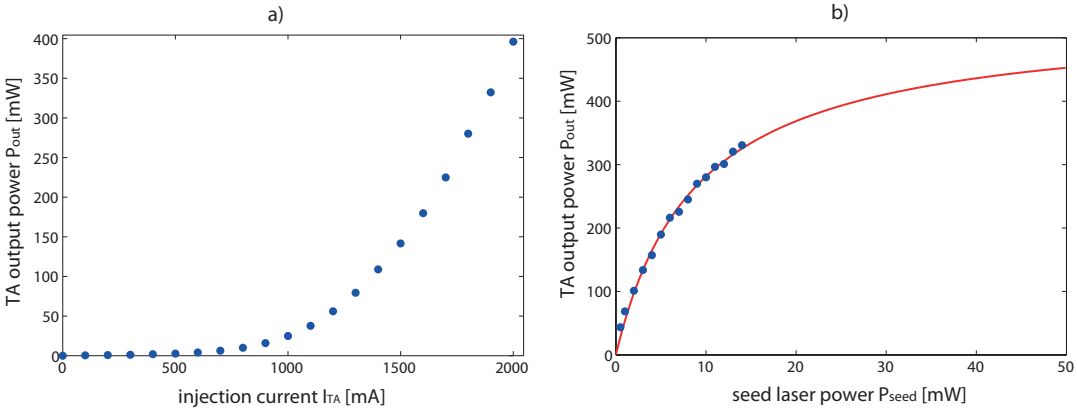

Figure 2.4: Left: TA output power vs. injection current with a constant seed laser power of 10mW. The seed laser power was measured once at the beginning and another time after the whole measurement to check if there have been any deviations. The injection current value was read out at the diode controller display.
Right: TA output power vs. seed laser power with a constant injection current of 1800mA. The circles depict measured data, the solid line is a fit of the type 2.1. No data points at higher seed laser power were taken since the seed providing laser diode could not be ran at higher output power without risk of damaging it.

To reach a reasonable signal for monitoring the small photodiode current is amplified with a current-to-voltage converter.
Figure 2.5 shows the dependency of the photodiode output signal on the seed laser power with and without TA turned on. The plot indicates a linear dependence of the photodiode signal on the seed laser power. It also shows that the output signal receives an offset when the TA is turned on. This increase of the signal is due to amplified spontaneous emission (ASE) of the TA diode. Since spontaneous emission occurs in all directions, a certain amount of this radiation reaches the right angle kinematic mirror and is scattered onto the photodiode. Since the slope of both signals does not change this indicates that the ASE is not influenced by the seed laser power but mainly determined by the injection current of the TA diode. The fact that the signal caused by the ASE is roughly as big as the monitoring signal from the transmitted seed laser makes it rather unpractical to use this monitoring for an interlock. A possible solution would be to replace the right angle mirror with a mirror of less reflectivity.

2.3.2 Beam quality

The beam quality of the TA output beam comes into play when the beam has to be coupled into a single mode fiber. The beams for the bichromatic cooling will be provided to the vacuum chamber via optical fibers. Single mode fibers are strongly

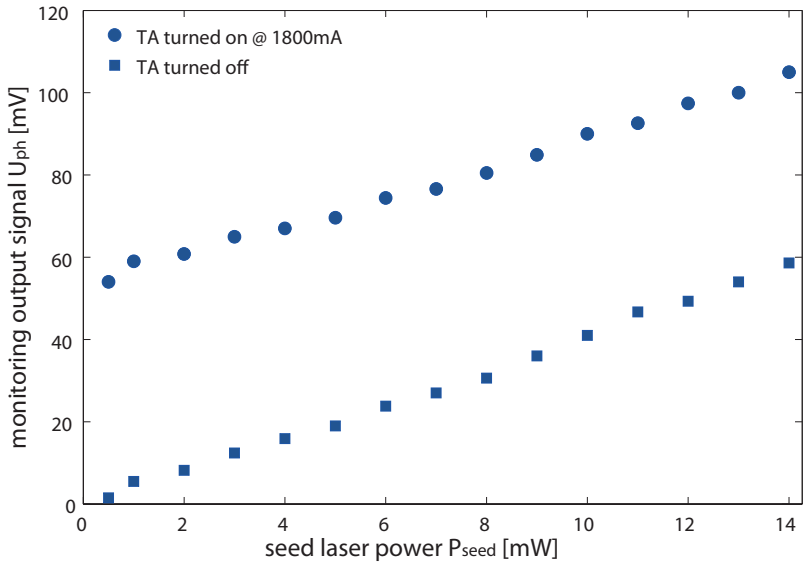

Figure 2.5: The plot shows the output signal of the monitoring circuit that was read out with an oscilloscope. The data points were taken as a function of seed laser power with and without TA turned on.
Between every measurement at least a few seconds had to be wait (time constant of the current-to-voltage converter: 1s).

mode selective meaning that the fibers excludes everything that deviates from the gaussian shape. The differences in divergency of the horizontal and vertical beam waist and also the ASE underground strongly distort the beam shape of the TA output beam.
The TA output beam deviates from the gaussian shape in being larger and having a more edged shape. Additionally, there is a broad ASE background. The TA output beam was optimized on highest coupling efficiency into a fiber using a fiber collimator (Schäfter Kirchhoff 60FC-4-A11-9) with focal length $f = 11$mm. The highest coupling efficiency reached so far is 36%. For future applications one should determine whether the coupling efficiency can be increased by using other fiber couplers since the loss due to coupling is a strongly limiting factor.

3 Generating an optical beating

Generating a light source that can be used as a π-pulse train was done with a quite technical approach. The goal is to create a light signal that fulfills two requirements. First it has to be a signal with a carrier frequency ω_{car} which corresponds to the atomic cooling transition. Second the signal has to have an amplitude modulation with frequency $\Delta\omega$ which can be tuned within the parameters of the experimental setup. Both can be achieved using light beating.

3.1 Adding monochromatic waves with frequency difference

Light beating can be explained in the theory of wave optics. A monochromatic wave can be described as the real part of a complex wave function [6]

$$\mathcal{E}(\vec{x},t) = \mathrm{Re}\{\left|\vec{E_0}\right| \exp(i(\omega t - \vec{k}\vec{x}))\} \quad , \tag{3.1}$$

where $\left|\vec{E_0}\right|$ is the amplitude of the electric field of the wave, ω the angular frequency and $\vec{k}$ the wavevector.
Consider now two light beams spatially overlapped and propagating in z-direction. Both waves have the same amplitude but different frequencies

$$\Delta\omega = \omega_2 - \omega_1 \qquad \Delta k = k_2 - k_1. \tag{3.2}$$

Since electromagnetic waves follow the principle of superpositon, the resulting wavefunction can be written as

$$\mathcal{E}(z,t) = \mathrm{Re}\{E_0 \exp(i(\omega_2 t - k_2 z + \Delta\phi)) + E_0 \exp(i(\omega_1 t - k_1 z))\} \qquad , \tag{3.3}$$

where $\Delta\phi$ represents the phase difference between both waves. By carrying out the operation and regrouping the terms equation 3.3 can be rewritten as

$$\mathcal{E}(z,t) = 2E_0 \cos\left(\frac{(\omega_2+\omega_1)t - (k_2+k_1)z + \Delta\phi)}{2}\right) \cos\left(\frac{\Delta\omega - \Delta k z + \Delta\phi)}{2}\right) \tag{3.4}$$

This expression represents a travelling wave with carrier frequency $\frac{\omega_2+\omega_1}{2}$ and amplitude modulating frequency $\frac{\Delta\omega}{2}$. The fact that an envelope of the signal arises

due to adding up two monochromatic waves with a certain frequency difference is called *beating*. Light beating provides exactly the both requirements mentioned earlier and thus is the principle that is used below.
An important point to mention here is that the frequency of the used light can not be measured in a direct way, since it is in the range of 10^{14} Hz. What indeed can be done in the laboratory is the measurement of the light intensity with a photodiode. The intensity of an electromagnetic wave is proportional to the squared absolute value of the complex envelope of the electric field [6]. For a monochromatic wave it is

$$I = \frac{|E_0|^2}{2\eta} \quad , \tag{3.5}$$

where η is the *impedance* of the medium the light is propagating through.

For an electromagnetic wave comprised of two frequencies like 3.3 the complex envelope varies in time thus the intensity for a fixed point in space is given as

$$I = \frac{1}{2\eta}(|E_1|^2 + |E_2|^2 + 2\,|E_1|\,|E_2|\cos(\Delta\omega t + \Delta\phi)) \quad , \tag{3.6}$$

where E_1 and E_2 denote the amplitude of each monochromatic wave and $\Delta\phi$ is the phase difference. This expression is very helpful. One can deduce the modulation frequency of the beating from it since the beat frequency is exactly the half of the frequency from the oscillating term in 3.6. Additionally from this expression one can make a prediction for the *visibility* [6]

$$\mathcal{V}_{vis} = \frac{I_{max} - I_{min}}{I_{max} - I_{min}} \quad , \tag{3.7}$$

which is a measure of the modulation depth of an interference pattern. Inserting in 3.6 into the visibility formula (where I_{max} is reached then the cosine is 1 and I_{min} then the cosine is -1) yields

$$\mathcal{V}_{vis} = \frac{2\sqrt{I_1 I_2}}{I_1 + I_2} = \frac{2\sqrt{I_2/I_1}}{1 + I_2/I_1} \quad , \tag{3.8}$$

where the formula was expanded so that the visibility can be expresssed in terms of the ratio between both intensities of each monochromatic wave.

3.2 Experimental setup

As should be seen from above the experimental challenge for generating a beating signal basically consists of two things. First, two beams with a frequency difference of $\Delta\omega$ have to be generated, second these two beams have to be overlapped spatially. In the course of this thesis an experiment was set up to achieve a beating. The following section is dedicated to this setup and describes its basics and also all essential details.

3.2.1 Overview

Figure 3.1 provides a schematic overview of the experimental setup and figure 3.2 shows a picture of the experimental setup in the laboratory. The light beam coming from the laser source first passes an anamorphotic lens pair to take care of the elliptically shaped laser beam than passes a faraday isolator to avoid backreflections from any optics back into the laser. A small amount of light intensity is deflected with a glass plate and used for spectroscopy to monitor that the wavelength of the laser is near the ^{40}Ar cooling transition. The rest of the laser beam passes a few more optics and enters the double pass AOM configuration. Here two beams with a frequency difference are generated and overlapped creating a light beating. This overlapped beam exits the double pass AOM configuration on the same path that the light enters it. After that the beating ist coupled into an optical fiber providing the seed laser for the TA. The beating signal can be observed before entering the fiber and also directly at the TA output. A few measurements have also been carried out with the detecting photodiode right behind the seed fiber.

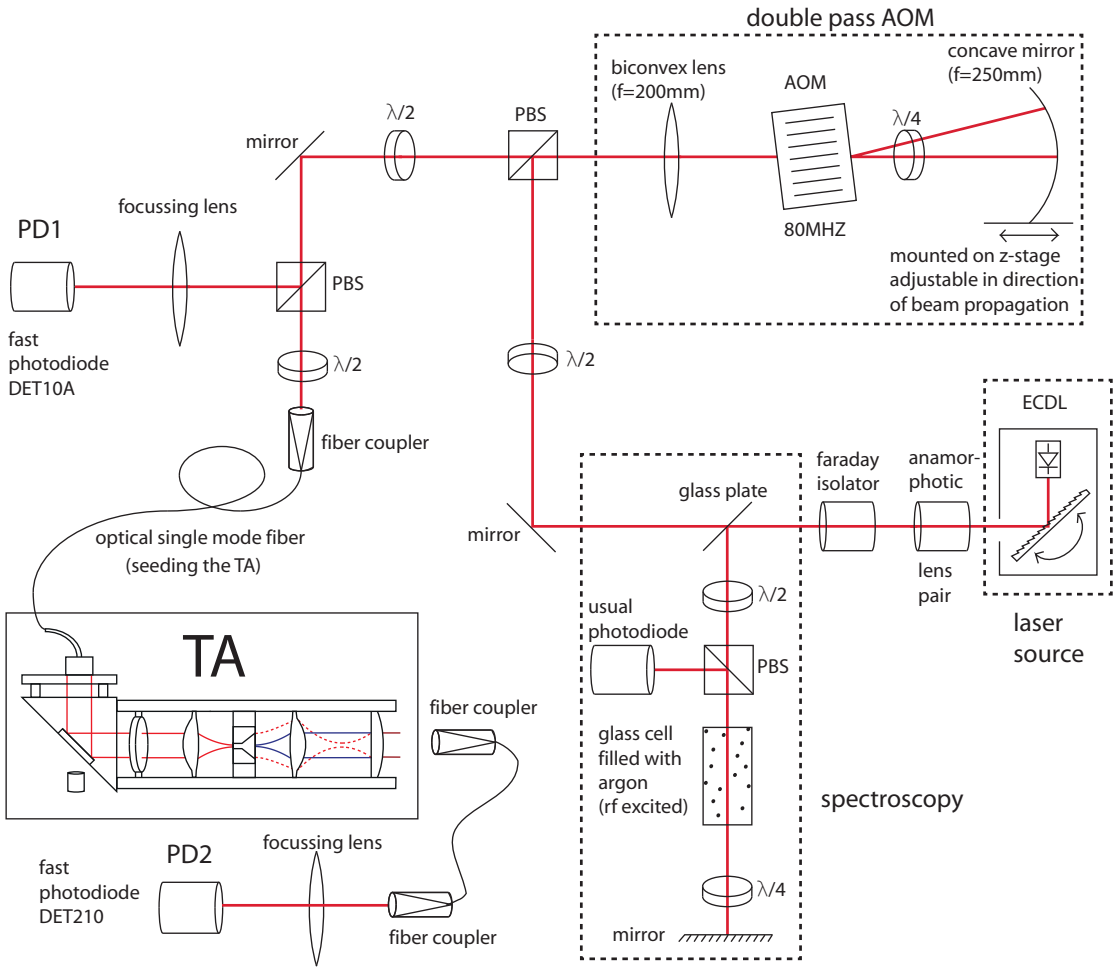

Figure 3.1: Sketch of the experimental setup.

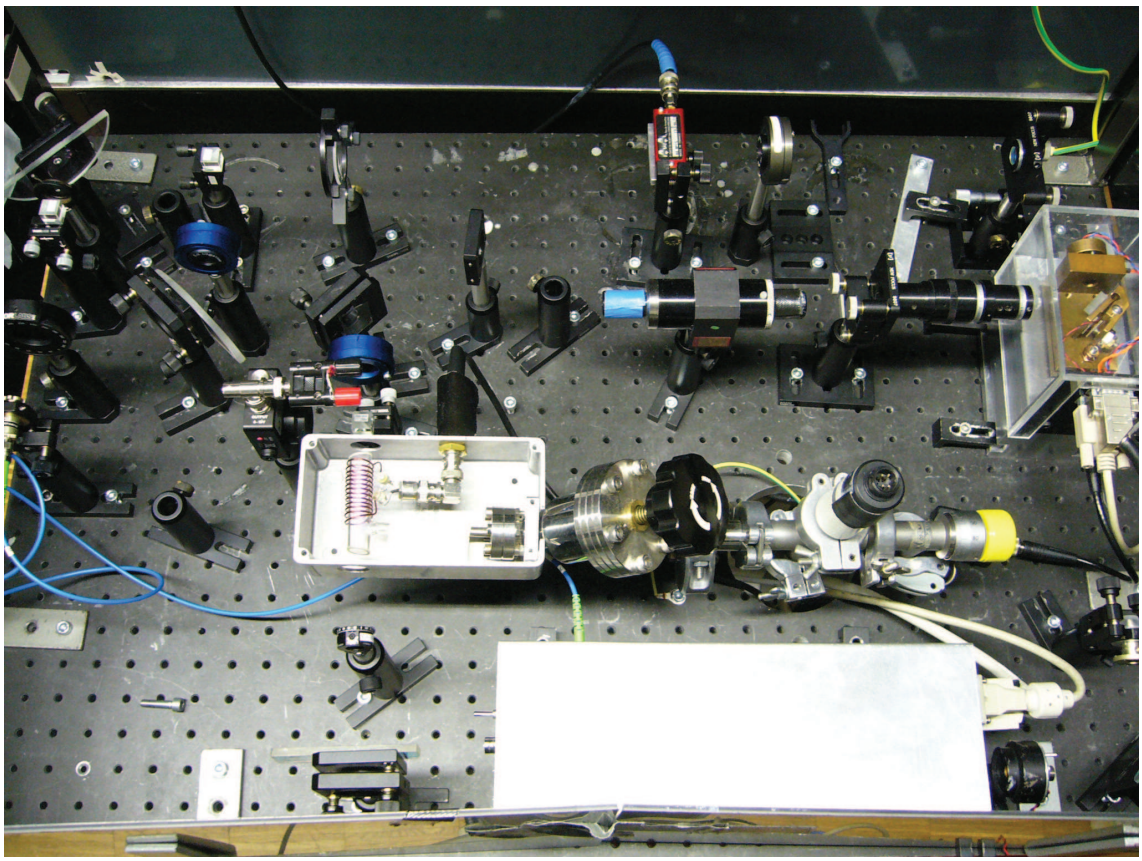

Figure 3.2: Picture of the experimental table with all important parts.

3.2.2 External Cavity Diode Laser - ECDL

The laser source used in the experiment is a diode laser with an external cavity [7]. This configuration basically consists of an optical grating and an usual laser diode that is operated with a current (see figure 3.3).
Choosing the position of the grating such that the 1-order diffraction angle and the icidence angle are the same is called Littrow configuration [7]. In that case the relation

$$2d\sin(\Theta) = n\lambda \tag{3.9}$$

holds. There d is the grating constant, Θ the diffraction angle, λ the wavelength of the diffracted light and n an integer describing the order of diffraction. Since the grating is dispersive by slightly changing the angle of the grating one can change the longitudinal mode of the light that is fed back into the external rasonator. The light that is coupled back mainly determines the wavelength of the amplified light in the resonator. So the wavelength of the output beam can be tuned by changing the position of the grating.

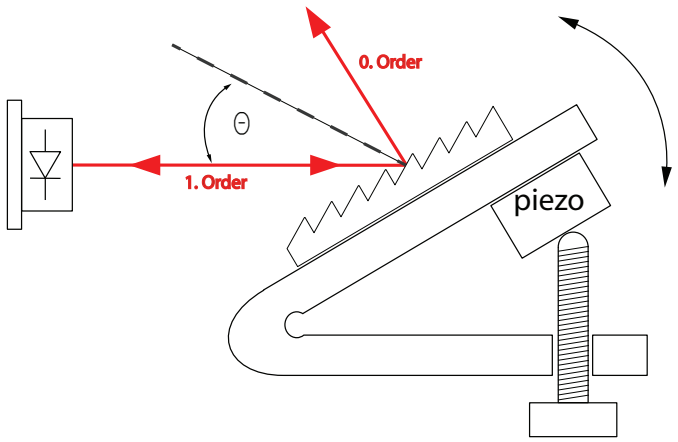

Figure 3.3: A sketch of the ECDL. The light emitted from the diode hits the grating and is diffracted. The 0th diffraction order is coupled out whereas the +1st diffraction order is fed back into the diode thus forming an external resonator. Picture taken from [5] (slightly adjusted).

For that purpose the angle and the horizontal position of the grating can be adjusted manually. Aditionally a piezo-electrical transducer is implemented that can change the angle of the grating very precisely.
For the experiment the wavelength of the ECDL was coarsaly adjusted to be at 811,754nm (measured with a wavemeter: Coherent WaveMaster) since it corresponds to the ^{40}Ar cooling transition [4]. For the later monitoring of the frequency the spectroscopy part of the experiment was used (see section 3.2.3).

3.2.3 Spectroscopy

The spectroscopy part is a setup using saturarion spectroscopy. It was used to ensure that the operating frequency was near the cooling transition and no mode hops occured. No active locking has beed performed. Scanning the grating of the ECDL leads to changes into the coupling efficiencies of the optical fibers. Due to that the spectroscopy check was performed before and after measurements.

3.2.4 Acousto Optical Modulator - AOM

Basic concept

For generating a second light beam with freqeuency shift $\Delta\omega$, that is used for the beating, an AOM is used in the experiment. An AOM is a device comprised of a crystal and a piezo-electric transducer bonded to it. The piezo can be driven with a RF-signal which generates a sound wave that propagates through the crystal. The presence of a sound wave alters the refractive index of the crystal. This fact is used to control light using sound waves [6] as illustrated in figure 3.4.

The sound wave indicated in the sketch acts as a diffractive grating for incident

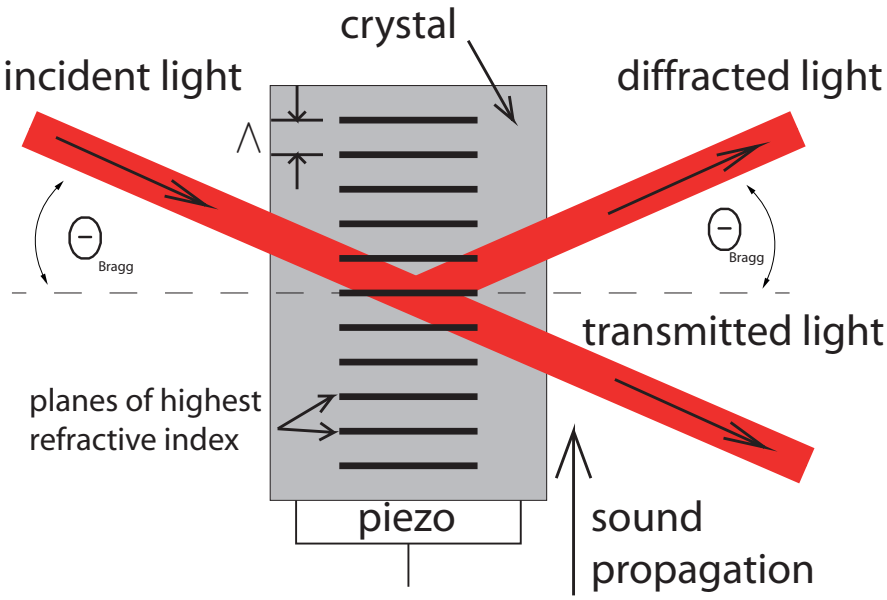

Figure 3.4: Sketch of an AOM device. A sound wave is applied to the crystal. The planes of highest refractive index have a periodicity of the wavelength of the sound wave Λ. Since the variation of the refractive index is slow compared to the optical period this variation can be regarded as static. To make the geometric considerations more descriptive the Bragg angle was drawn in an exaggerated manner. The Bragg angle for the used setup is in the range of mrad (see 3.2.4).

light when Θ satisfies the Bragg condition [6]

$$\sin\Theta_{Bragg} = \frac{\lambda}{2\Lambda} \quad , \tag{3.10}$$

where λ is the wavelength of the incident light. A configuration of the AOM as it is shown in figure 3.4 is called single pass.
The diffraction of light is accompanied by a frequency shift. This shift can be explained in a quantum interpretation of the problem,where light is considered as a stream of photons with energy $\hbar\omega_l$ and momentum $\hbar k_l$ and the sound wave is treated as a stream of phonons each of energy $\hbar\omega_s$ and momentum $\hbar k_s$ [6]. From energy conservation $\hbar\omega_{new} = \hbar\omega_l \pm \hbar\omega_s$ follows that the frequency of the diffracted beam is shifted by $\pm\omega_s$. An upshift of frequency means that a phonon is destroyed and transfers its energy to the new photon. This is the case when the light beam is diffracted into the +1st diffraction order. A downshift of frequency means that the photon loses energy and a new phonon is generated. This is the case when the light beam is diffracted into the -1st diffraction order. The 0th diffraction order is just transmission through the crystal. In that case no interaction between photons and phonons takes place and the frequency of the transmitted beam stays unchanged.

One should note here that while running an AOM also diffraction into higher orders takes place. But for the purpose of clarity and because their contribution is negligible in the following only the ±1st and 0th diffraction order are considered.

Double pass configuration

As pointed out, an AOM in the single pass configuration can be used to generate two different beams with a frequency shift ω_s. But these two beams leave the AOM at different angles. To create a beating these two beams have to be overlapped spatially. In the experiment a double pass configuration was used to perform this overlapping. In this configuration a concave mirror is placed behind the AOM such that the output beams from the AOM are reflected back so that they pass the AOM a second time (see figure 3.5). After the double pass configuration there are four light beams with four different frequencies:

- The beam that is diffracted into the 0th order at the first and the second pass. It is denoted (0,0) and has the frequency ω_l.
- The beam that is diffracted into the 1st order at the first pass and also into the 1st order at the second pass. It is denoted (1,1) and has the frequency $\omega_l + 2\omega_s$.
- The beam that is diffracted into the 1st order at the first pass and into the 0th order at the second pass. It is denoted (1,0) and has the frequency $\omega_l + \omega_s$.
- The beam that is diffracted into the 0th order at the first pass and into the -1st order at the second pass. It is denoted (0,-1) and has the frequency $\omega_l - \omega_s$

Beams (0,0) and (1,1) are overlapped spatially as well as beams (1,0) and (0,-1).

In a simplified ray optic picture there is a point z_0 in the AOM from that the different diffraction orders originate. It is important to place the curved mirror such that the center of curvature of the mirror coincides with the point z_0. Only then the beams are perfectly overlapped as mentioned above. Figure 3.6 shows the case where the mirror is positioned too far away. In this case the beams are not overlapped any more. To overcome this problem the mirror is mounted on an adjustable z-stage so that the distance between the AOM and the mirror can be optimized.
In the setup the overlapping beams (0,0) and (1,1) were used to generate the beating. For future applications one should consider whether the beams (1,0) and (0,-1) can also be used as a part of the bichromatic cooling setup.

Technical details

The AOM that was used in the experiment (AA.MO.15) has an active aperture of 1mm × 2mm. The incoming laser beam that has a beam waist of about 2mm is focused by a spherical lens (f=200mm) such that the beam waist in the focus fits within the active region. The used curved mirror has a curvature radius of 250mm. The signal that drives the AOM is generated with a function generator (Agilent

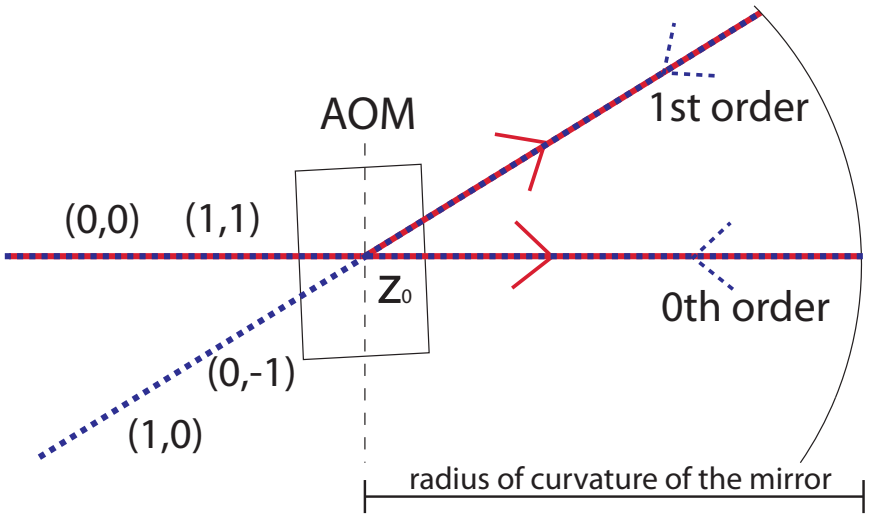

Figure 3.5: Sketch of the double pass configuration based on a consideration of ray optics. The red straight lines represent the light beams that pass the AOM once. The blue dotted lines represents the light beams that are reflected from the mirror and pass the AOM a second time. The tuple (i,j) represents the beam that was diffracted into the i-th order first passing the AOM and into the j-th order second passing the AOM.

33250A). It is a 80MHz sine waveform that is amplified with a 1W power amplifier (ZHL 1A).
The AOM has a $PbMoO_4$ crystal (lead molybdate) with an acoustic velocity of $3630\frac{m}{s}$. Inserting this into equation 3.10 yields $\Theta_{Bragg} \approx 9$mrad.
The setup was optimized to have a ≈ 1.5 mW beat signal after coupling into a fiber. This is far below the optimum seed power for the TA, however in this regime the amplification can be regarded as linear (see figure 2.4 right)

3.3 Beating signal

The beating is observed by measuring its intensity with fast photodiodes (Thorlabs DET210 and DET10A, risetime: 1ns). The signal from the photodiodes is displayed by an oscilloscope (Tektronix TDS 2024B, bandwidth 200MHz) and can be read out with a computer. From that conclusions about the properties of the beating can be deduced. In the following, two questions of major interest are focused:

1. How does the phase of the beating vary in time and how is it influenced by the TA?

2. What conclusion can be drawn from the visibility of the beating signal?

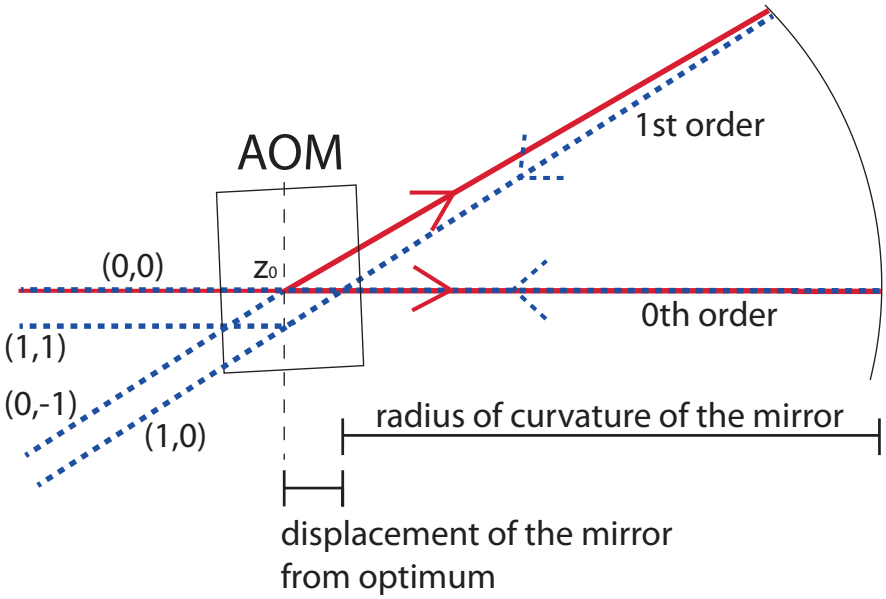

Figure 3.6: A sketch of the double pass configuration where the mirror is placed too far away. By that the two reflected beams do not meet at z_0 where they originate from. So they reach the active region of the AOM at different points and compared to figure 3.5 the beams are not spatially overlapped.

3.3.1 Phase

To compare the phase of the beating before and after the TA the two signals are displayed on the oscilloscope. The signal detected with PD1 represents the unamplified beating and the signal detected with PD2 represents the amplified beating. Figure 3.7 shows the two signals directly read out from the oscilloscope. Both signals are cosine waveforms as one would expect from equation 3.6. The fact that both signals can be triggered with one frequency already indicates that both waveforms have the same frequency. The huge difference in the offset of both signals will be discussed later, for evaluating the phase the exact offset is not necessary to be known.
A first test, how the phase behaves, is to slightly tap the curved mirror. By that the phase of both signals fastly changes. This is explained by the fact that the two beams that are reflected from the curved mirror are not yet overlapped so that a change of the relative path length by an optical wavelength ($\approx 0.811 \mu m$) changes the relative phase by 2π. Tapping the mirror does perform such changes and thus the displayed signal switches back and forth on the time axis. From this first observation the TA seems to conserve quick changes in the phase relation of its seed. However, to measure long term phase changes the oscilloscope was read out every 10 seconds over a time span of several hours. The phases of each single measurement are determined by applying a least squares fit of the function

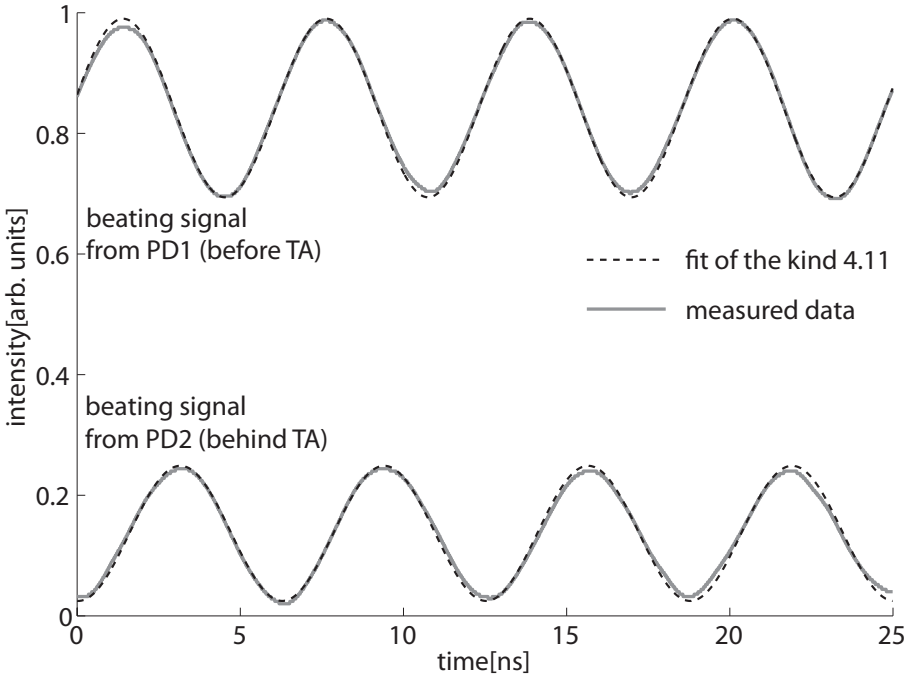

Figure 3.7: Intensity of the beating signals as a function of time. The data is acquired by directly reading out the oscilloscope display. The oscilloscope is triggered with the 80MHz signal that drives the AOM. The amplitude of the two signals have been adjusted to be roughly equal with the power splitter in front of the seeding fiber of the TA.

$$f(t) = A\cos(2\pi\omega t + \phi) + O \qquad , \tag{3.11}$$

where A is the amplitude, ω the angular frequency, ϕ the phase and O the offset. The phase for each beating is extracted from the fit parameters and presented in figure 3.8.

Both phases of figure 3.8 experienced a long term drift in the first hour. After that they had some short time spikes which seem to be correlated. Taking the difference of both signals shows that the difference stayed rather constant over the whole measuring time. Taking the difference of both phases also reduced the noise, meaning that some of the fast fluctuations are correlated. This correlated noise is likely caused by the fluctuations of the trigger signal. The fluctuations in phase difference are about 3% which probably can be attributed to the readout accuracy of the oscilloscope and the error of the fit routine. Summing up one can say, that the TA conserves the phase relation of the seed laser. It should be noted here, that the polarization maintaining coupling of the fiber using a half-wave plate greatly enhanced the stability of the measurement. Compared to earlier measurements the long term fluctuations and also spontaneous shifts in phase could be avoided.

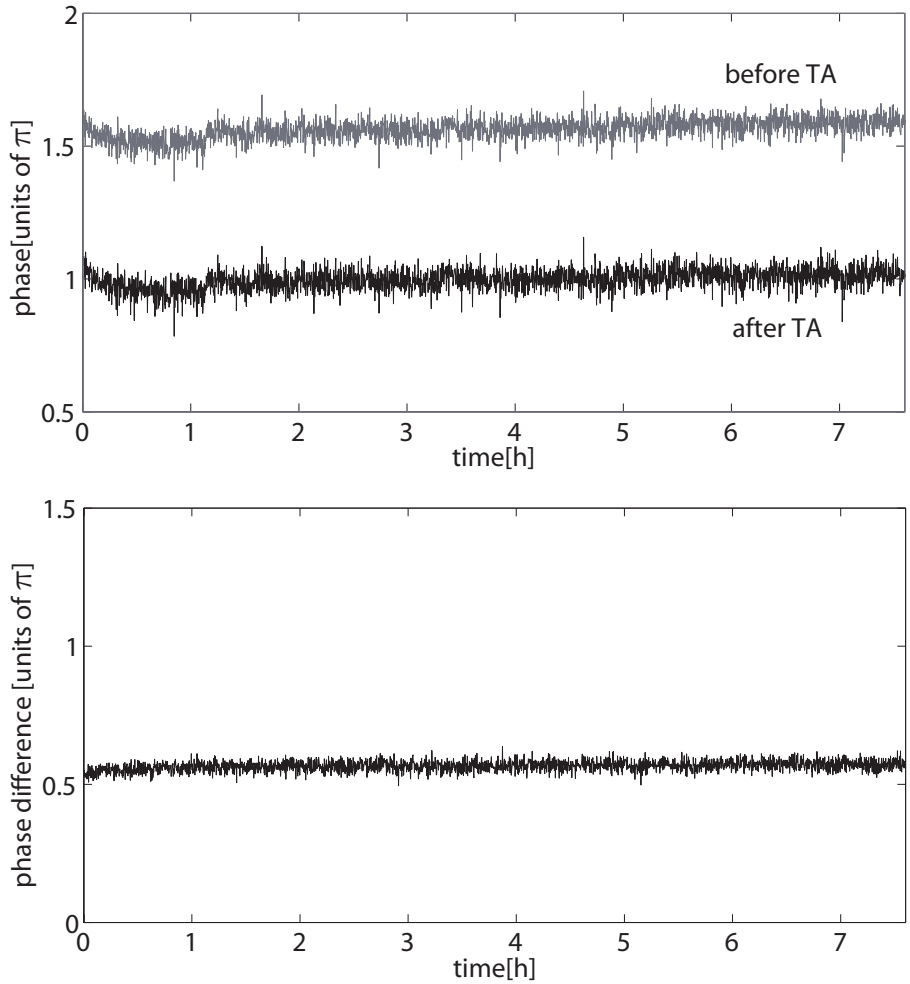

Figure 3.8: Top: Phase of each beating signal as a function of time. Bottom: Phase difference between both beatings by subtracting the two signals from the top plot from each other.

3.3.2 Modulation depth

One thing that is apparent from figure 3.7 is the huge offset of the beating detected with PD1 compared to the one detected with PD2. After this signal was coupled into a fiber the relative offset greatly reduced. This shows that the two beams which leave the double pass configuration are not perfectly overlapped. The coupling into a fiber excludes the parts of the beam that do not contribute to the beating. Still an offset remains and to check whether it is caused by the measuring instruments (photodiode, oscilloscope) a faster photodiode (UltraFast-20-SM, risetime < 12ps) and an oscilloscope with higher bandwidth (Picoscope9201A, bandwidth 12GHz) were used. Even using the enhanced equipment still an offset of about 10% compared to the maximum value occured.
To make a more systematic statement about the offset the visibility of the amplified

beating was measured for different power balancings of the two beams. I_{max}, I_{min}, I_0 and I_1 are measured, where I_0 is the intensity detected on the photodiode, when the 1st diffraction order at the AOM is blocked and I_1 accordingly when the 0th diffraction order is blocked. The ratio I_1/I_0 of the intensities of the two light beams is varied from 1 down to 0 by adjusting the diffraction of the AOM accordingly. Figure 3.9 shows the results of this measurement.

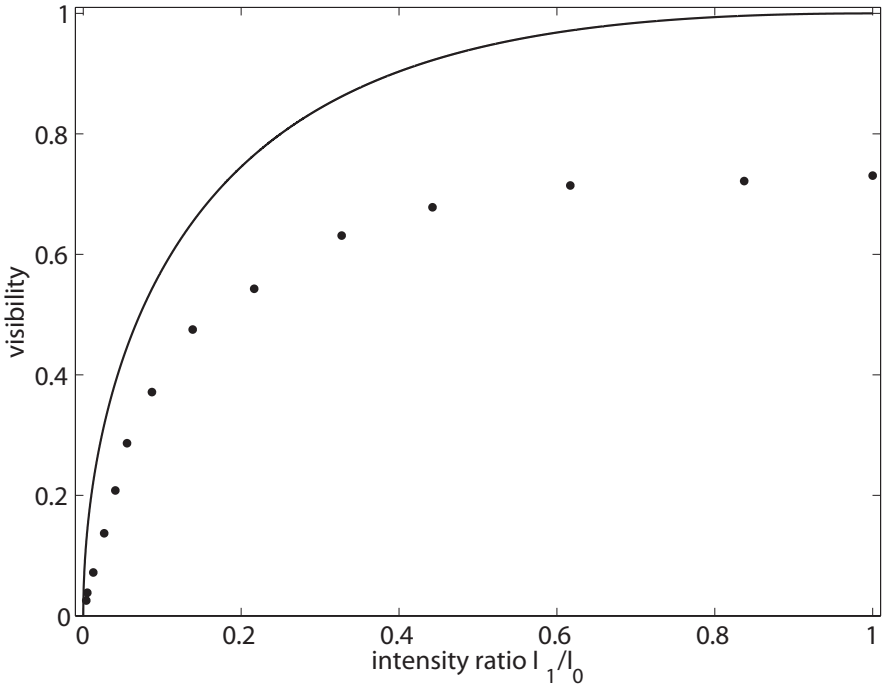

Figure 3.9: Data points of the measurements and a plot of the theoretical prediction 3.8

The experimental data is clearly not described by equation 3.8 since the visibility does not reach 1. As the ratio of intensities can be tuned continously between 0 and 1 there has to be another explanation for the remaining offset. A possible reason for this could be that the measured intensities I_0 and I_1 also contain an amount of intensity that does not contribute to the beating signal and thus remains as an offset even for $I_1/I_0 = 1$.
Assuming the offset arises due to that, equation 3.6 has to be corrected to

$$I = \frac{1}{2\eta}(\hat{\mathrm{I}}_0 + \hat{\mathrm{I}}_1 + 2\sqrt{I_0 I_1}\cos(\Delta\omega t + \Delta\phi)) \qquad , \tag{3.12}$$

where $\hat{\mathrm{I}}_{0/1} = I_{0/1} + c_{0/1}I_{0/1}$ indicates the intensity is comprised of $I_{0/1}$ that contributes to the beating and $c_{0/1}I_{0/1}$ that does not. $\hat{\mathrm{I}}_{0/1}$ is the value that is measured with the diode, it appears in the dc term of equation 3.12 whereas in the modulating part solely $I_{0/1}$ appears.
Inserting this new adapted formula into 3.7 yields the corrected visibility

$$\mathcal{V}_{corrected} = \frac{2\frac{1}{c+1}\sqrt{\hat{I}_1/\hat{I}_0}}{1+\hat{I}_1/\hat{I}_0} \quad , \tag{3.13}$$

where the parameter c is assumed to be $c = c_0 = c_1$ and the term is expressed in terms of $\frac{I_1}{I_0}$.The assumption $c = c_0 = c_1$ is made because both beams that generate the beating are generated under similar circumstances, thus an additional non interfering intensity part is likely produced by the same effects.
This corrected formula is applied to the data via a least-squares-fit. The fit yields $c = 0.41$ what means that according to the adjusted theory 29% of each beam does not contribute to the beating. The fit is shown in figure 3.10.

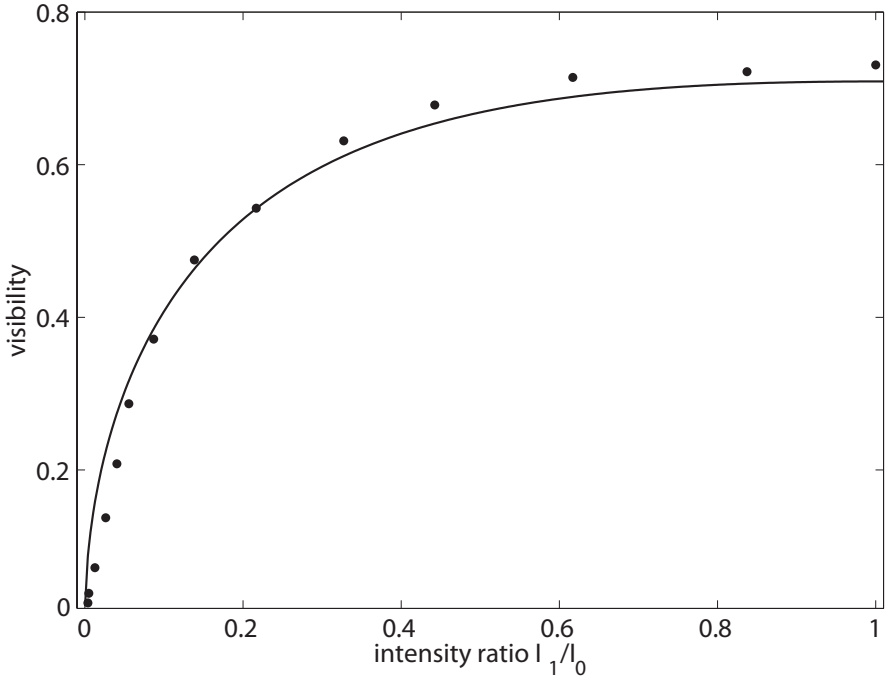

Figure 3.10: Experimental data points with a fit of the kind 3.13

It can be seen that the equation for the corrected visibility describes the data much better than equation 3.8. But the residuuals of the fit do not scatter randomly around 0. They tend to be below zero for $\frac{I_1}{I_0}$<0.2 and above zero vor $\frac{I_1}{I_0}$>0.2. An indication that the theory does not explain all the details of the problem. To make convincing statements more data has to be taken.
At least this observation gives a hint how the offset in the intensity of the beating can be interpreted. For further application of this setup the origin of this upcoming offset should be investigated. Possible explanation for an not interfering intensity part in the beams could be that the two beams that are supposed to generate the beating contain certain parts of light with different polarization. Since electromagnetic waves with perpendicular polarization to each other do not interfere this explanation would fit quite well with the statemet above. However, the beams pass a polarizing beam

splitter several times which represents a good polarization filter. An argument that indicates the unlikelihood of the offset being produced by polarization issues.

4 Conclusion and outlook

It was shown that an optical beating can be generated with the presented AOM configuration. It was further shown that the implemented taperded amplifier amplifies the optical beating while maintaining the phase relation and the visibility of the incoming beating signal.
However, certain shortcomings of the present setup could be identified. Only ∼25% of the laser light entering the AOM could be distributed to the overlapping diffraction orders that contributed to the measured beating signal. Furthermore, only ∼30% of this beating signal could be coupled into a fiber. The low fiber coupling efficiency can be attributed to the imperfections of the beam overlap. This explanation is confirmed by the large offset that was observed in the beating signal before the fiber. Even the beating signal leaving the fiber still shows an offset indicating that despite fiber coupling a non-beating component remains. Whether this offset has an effect on the bichromatic cooling process, needs further investigation. The overlap of the two beams might be further improved by more careful alignment of the optics, especially the position of the curved mirror and the focussing lens before the AOM.
Another shortcoming of the present setup is the insufficient laser power obtained after fiber coupling the TA output. On the one hand this problem can be addressed by employing a seed laser with higher power. On the other hand the output power of the TA can be increased by running the injection current closer to its specified maximum value of 3A.
In the farer future, one may think of modulating the injection current of the TA according to the incoming beating. This way, the injection current could be increased to even 6A, since the duty cyle covers only half of the time. Fibre coupled output powers of up to ∼1W may be achievable by doing so.

Bibliography

[1] Matthew Jeremiah Partlow. *Bichromatic Collimation to Make an Intense Helium Beam*. PhD thesis, Stony Brook University, 2004.

[2] Harold J. Metcalf and Peter van Straten. *Laser cooling and trapping*. Springer, New York ; Berlin ; Heidelberg [u.a.], 1999.

[3] Daniel Thomas Stack. *Optical Forces from Periodic Adiabatic Rapid Passage Sequences on Metastable Helium Atoms*. PhD thesis, Stony Brook University, 2012.

[4] F. Ritterbusch. Realization of a collimated beam of metastable atoms for atta of argon 39. Master's thesis, Faculty of Physics and Astronomy, University of Heidelberg, 2009, www.matterwave.de.

[5] M. Henrich. Design and realization of a laser system for atta of argon 39. Master's thesis, Faculty of Physics and Astronomy, University of Heidelberg, 2010, www.matterwave.de.

[6] B. E. Saleh and M. C. Teich. *Fundamentals of photonics*. Wiley, Hoboken, N.J., 2007.

[7] Sven-Olaf Soltau. Aufbau eines diodenlasersystems fuer eine magneto-optische falle mit metastabilem argon. Master's thesis, Universitaet Konstanz, Lehrstuhl Prof. Dr. J. Mlynek, 1995.

Erklärung

Ich versichere, dass ich diese Arbeit selbstständig verfasst und keine anderen als die angegebenen Quellen und Hilfsmittel benutzt habe.

Heidelberg, den 06.08.2013,